Available online at www.sciencedirect.com
ScienceDirect
Biosensors and Bioelectronics 23 (2008) 1397–1403
BIOSENSORS & BIOELECTRONICS
www.elsevier.com/locate/bios

Detection of viral bioagents using a shear horizontal surface acoustic wave biosensor

M. Bisoffi [a,*], B. Hjelle [b], D.C. Brown [b], D.W. Branch [c], T.L. Edwards [c], S.M. Brozik [c], V.S. Bondu-Hawkins [b], R.S. Larson [b]

[a] *Department of Biochemistry and Molecular Biology, The University of New Mexico School of Medicine, Albuquerque, NM, USA*
[b] *Department of Pathology, The University of New Mexico School of Medicine, Albuquerque, NM, USA*
[c] *Sandia National Laboratories, Albuquerque, NM, USA*

Received 19 July 2007; received in revised form 15 November 2007; accepted 11 December 2007
Available online 3 January 2008

Abstract

Viruses are of high medical and biodefense concern and their detection at concentrations well below the threshold necessary to cause health hazards continues to be a challenge with respect to sensitivity, specificity, and selectivity. Ideally, assays for accurate and real time detection of viral agents would not necessitate any pre-processing of the analyte, which would make them applicable for example to bodily fluids (blood, sputum) and man-made as well as naturally occurring bodies of water (pools, rivers). We describe herein a robust biosensor that combines the sensitivity of surface acoustic waves (SAW) generated at a frequency of 325 MHz with the specificity provided by antibodies for the detection of viral agents. A lithium tantalate-based SAW transducer with silicon dioxide waveguide sensor platform featuring three test and one reference delay lines was used to adsorb antibodies directed against either Coxsackie virus B4 or the category A bioagent Sin Nombre virus (SNV), a member of the genus Hantavirus, family *Bunyaviridae*, negative-stranded RNA viruses. Rapid detection (within seconds) of increasing concentrations of viral particles was linear over a range of order of magnitude for both viruses, although the sensor was approximately 5×10^5-fold more sensitive for the detection of SNV. For both pathogens, the sensor's selectivity for its target was not compromised by the presence of confounding Herpes Simplex virus type 1. The biosensor was able to detect SNV at doses lower than the load of virus typically found in a human patient suffering from hantavirus cardiopulmonary syndrome (HCPS). Further, in a proof-of-principle real world application, the SAW biosensor was capable to selectively detect SNV agents in complex solutions, such as naturally occurring bodies of water (river, sewage effluent) without analyte pre-processing. This is the first study that reports on the detection of viral agents using an antibody-based SAW biosensor that has the potential to be used as a hand-held and self-contained device for rapid viral detection in the field.

Keywords: SAW; Biosensor; Antibody; Virus; Category A bioagent; Hantavirus

1. Introduction

Recently, there has been a heightened interest in developing rapid and reliable methods of detection of micro-organisms involved in bioterrorism, food poisoning, and clinical problems. Biosensors are devices under intense development to achieve these goals and a number of different types of transduction modes are currently investigated, including electrochemical, optical, thermal, and acoustic (Deisingh and Thompson, 2004). Shear horizontal surface acoustic wave (SH-SAW) devices that are based on horizontally polarized surface shear waves (HPSSW) enable label-free, sensitive and cost-effective detection of biomolecules in real time and have been used for the detection of bacteria and viral DNA (Berkenpas et al., 2006; Branch and Brozik, 2004; Moll et al., 2007). A SAW device typically has a planar electrode structure consisting of a piezoelectric substrate containing inter-digital transducers (IDTs) (Branch and Brozik, 2004). An often used substrate compound that meets many of the required conditions for successful HPSSW generation is lithium tantalate ($LiTaO_3$) (Branch and Brozik, 2004; Martin et al., 2004). Applying an alternating voltage via the IDTs at high frequency (typically from 80 to 400 MHz), HPSSW

* Corresponding author at: Department of Biochemistry and Molecular Biology, University of New Mexico School of Medicine, MSC08 4670, 1 University of New Mexico, Albuquerque, NM 87131, USA. Tel.: +1 505 2728157; fax: +1 505 2726587.
E-mail address: mbisoffi@salud.unm.edu (M. Bisoffi).

0956-5663/$ – see front matter © 2007 Elsevier B.V. All rights reserved.
doi:10.1016/j.bios.2007.12.016

are generated on the substrate. These HPSSW result in a specific resonance frequency that is characteristic for the substrate surface wave velocity. The frequency is sensitive to measurable changes on the sensor surface, for example caused by specific biological interactions.

The present study deals with the detection of viruses by SAW. Initially, we used Coxsackie virus, a member of the enterovirus family, which also includes polioviruses and hepatitis A virus (Palacios and Oberste, 2005). Coxsackie virus infections are usually not of major health concern and possible fevers, headaches, and muscle aches typically self-resolve after several days. Occasionally however, Coxsackie virus can cause serious infections, such as hand, foot and mouth disease, viral meningitis, encephalitis, myocarditis, and hepatitis, especially in newborns (Frydenberg and Starr, 2003; Tam, 2006). Our primary objective is the Sin Nombre virus (SNV), a hantavirus member of the *Bunyaviridae* family of RNA viruses and a category A agent as defined by the National Institute of Allergy and Infectious Diseases (NIAID; www.niaid.nih.gov). SNV is transmitted by its reservoir host *Peromyscus maniculatus*, the deer mouse. Transmission happens by inhalation of aerosolized feces, urine, or saliva from the infected mice (Jay et al., 1997). The illness that ensues, hantavirus cardiopulmonary syndrome (HCPS), is characterized initially by mild flu-like symptoms, followed by rapid progression to respiratory distress, and can be fatal (Hjelle, 2002; Mertz et al., 2006). There is no established therapeutic regimen and treatment is only supportive. Preventive methods include attempts to minimize contact with the rodents since elimination of the virus is not realistic. Although human infections with hantaviruses are on the rare side, these agents have been classified by the Center of Disease Control (CDC) as potential agents for biologic terrorism due to their relative ease of production, the high susceptibility of large populations, and the limited treatment and vaccination strategies (Bronze et al., 2002).

We report here on the development and preliminary use of an SH-SAW biosensor able to detect category A viral agents operating at an input frequency of 325 MHz. This work extends our previous efforts into the design of SH-SAW biosensors for the detection of microorganisms (Branch and Brozik, 2004). We show that this device is sensitive and highly selective for its specific target. We also provide data in support of the biosensor's high reproducibility and its use in a real world scenario mimicking the exposure of an urban population to a viral agent, such as for example through the water system. Our results indicate that this detection platform is highly versatile and robust and has significant medical or defense use.

2. Materials and methods

2.1. Fabrication of the 325 MHz SH-SAW sensor

2.1.1. Wafer preparation and lithographic deposition of IDT layer

The SH-SAW device was fabricated using metal evaporation and lift-off plasma enhanced chemical vapor deposition (PECVD), and reactive ion etching (RIE) techniques on a 36° *y*-cut, *x*-propagating lithium tantalate ($LiTaO_3$) crystal wafer of 510 μm thickness and 100 mm diameter. The wafer was cleaned in a barrel asher (PVA Tepla, Asslar, Germany) for 5 min, 600 W power and 900 mTorr of O_2, followed by dipping in 1 vol.% hydrofluoric acid (HF) for 3 min, and rinsing in a cascade bath until the resistivity of the water was greater than 12 MΩ cm followed by drying under N_2. The wafer layout was designed to include four IDT patterns with sets of transducers and delay lines. AZ2020 (AZ Electronic Materials, Branchburg, NJ, USA) negative-tone photoresist (PR) was applied using a spin coater with a Gyrset lid (Karl-Suss, Waterbury Center, VT, USA) at 1300 rpm and 3000 rpm/s for 30 s to achieve a thickness of 2.0 μm. The wafer was baked on a hotplate for 60 s at 110 °C and cooled to room temperature on a metal surface. Because of the pyroelectric nature of $LiTaO_3$ it was necessary to remove residual electric charge by dipping the wafer in de-ionized water and drying under N_2. The PR was exposed to i-line UV light at 365 nm for 6 s at 14 mW/cm^2. The wafer was re-baked on a hotplate at 110 °C for 60 s followed by a 1 min developing time in a 300 MIF developer (AZ Electronic Materials) and rinsing in de-ionized water. The wafer was metallized with 5000 Å aluminum using an electron-beam evaporator (Temescal, Wilmington, MA, USA). The deposition rate was 3 Å/s for 500 Å and then 5 Å/s for 4500 Å. The wafer was placed in an acetone bath to lift off the PR and excess aluminum. An acetone spray was used to remove the PR between the IDT fingers, followed by rinses in methanol, isopropyl alcohol, and de-ionized water. This procedure was repeated for the metallization of the ground plane, buss lines, and contact pads.

2.1.2. Deposition of the waveguide layer and final preparation

A 5000 Å silicon dioxide (SiO_2) film was deposited onto the entire wafer using PECVD (Oerlikon Versaline, Pfaeffikon, Switzerland) at 150 °C for 410 s. The oxide was coated with hexamethyldisilazane (HMDS) in a vacuum oven at 100 °C for 30 min. AZ4330 positive-tone PR (AZ Electronic Materials) was spin coated onto the wafer at 2000 rpm and 3000 rpm/s for 30 s. The wafer was baked on a hotplate at 90 °C for 90 s, exposed for 48 s at 20 mW/cm^2 (at 400 nm), and developed in a 300 MIF developer for 3 min. A photoresist mask was used to "open" the SiO_2 and expose the electrical contact pads. The SiO_2 was etched by RIE (Oerlikon Versaline) for 1500 s (p = 40 mTorr, CHF3 = 45 sccm, O_2 = 5 sccm, P = 125 W, DC bias = 712 V). The wafer was diced using a resinoid dicing blade. The PR was removed from the individual die by rinsing in acetone, methanol, and isopropanol.

2.2. Virus production and preparation

Viral work was conducted in Biosafety Level 2 (Coxsackie virus B4) or Level 3 (SNV) facilities at the University of New Mexico School of Medicine. The JVB strain of Coxsackie virus B4 was purchased from ATCC (Manassas, VA, USA). Buffalo Green Monkey Kidney (BGMK) cells were purchased from Diagnostic Hybrids, Inc. (Athens, OH, USA). BGMK cells were grown to confluency in DMEM, 2 mM L-glutamine, 10 mM

HEPES, 26.8 mM sodium bicarbonate, and 10% fetal bovine serum. After removal of culture media, BGMK cells were inoculated with Coxsackie virus B4 for 1 h at room temperature and grown in a serum free media, Opti PRO SFM (GIBCO, Grand Island, NY, USA) supplemented with 4 mM L-glutamine. Upon reaching 100% cytopathic effect (CPE), the media was centrifuged in a sealed rotor for 5 min at 3000 rpm and the supernatant was stored at −20 °C. The viral titer was determined by serial dilution and growth in BGMK cells. The virus was inactivated with 2.0 Mrad of gamma radiation using a Gammacell 40 (Atomic Energy of Canada, Ltd., Kanata, Ontario, Canada) and concentrated by lyophilization and resuspension in distilled water.

SNV particles were purified from the supernatant of VeroE6 monkey kidney cells (ATCC) infected with SNV at a multiplicity of infection of 0.1 for 1 h. After 9 days the media was subjected to ultracentrifugation using Optiprep density gradients in phosphate buffered saline (PBS) (Axis-Shield, Norton, MA) and the isolated virus was inactivated by UV. The amount of SNV particles was quantified by determining the SNV nucleocapsid (SNV-N) protein concentration (not shown). SNV particle number was calculated based on the following parameters pertaining to the SNV-N protein: SNV-N has a mass of 50 kDa; thus 1 mol $(6.02 \times 10^{23}) = 50{,}000$ g; thus one SNV-N protein $= 8.3 \times 10^{-11}$ ng. There are $\sim 10^5$ SNV-N proteins per SNV particle; thus 8.3×10^{-6} ng of SNV-N = one SNV particle. Using these calculations, 1 ng of SNV-N protein corresponds to ∼120,000 SNV particles. Purified Herpes Simplex virus type 1 (HSV-1) was a kind gift of Dr. Stephen Young at TriCore Laboratories (Albuquerque, NM, USA).

2.3. Preparation of antibodies and adsorption to the SAW biosensor

The IgG2a isotype monoclonal antibody (mAb) directed against the JVB strain of Coxsackie virus B4 was produced by the 204-4 hybridoma cell line (ATCC). The mAb was labeled with biotin using the EZ-Link NHS-PEO Solid Phase Biotinylation Kit and Spin Column featuring the SwellGel Disk technology (Pierce, Rockford IL, USA). The mAb was added to the gel at 2 mg/ml for 10 min followed by incubation in NHS-PEO4-Biotin for 30 min at room temperature and column spinning. The biotin labeled antibody was eluted from the column with 0.2 M Imidazole in PBS. Single chain Fv antibodies (scFv) directed against SNV have been previously selected from a phage antibody library, and are specific for the SNV-G1 glycoprotein exerting no cross-reactivity with glycoproteins from other hantaviruses (Velappan et al., 2007). These scFv antibodies were left unmodified and directly adsorbed to the biosensor.

The SAW devices were cleaned in acetone, methanol, and isopropanol, then treated by ultrasonication in 95% ethanol, rinsed in distilled water, followed by exposure to UV-ozone for 10 min in a UVOCS UV-ozone cleaner (UVOCS Inc., Montgomeryville, PA, USA). For the antibody directed against the Coxsackie virus B4, the oxide layer of the test delay lines of the SAW device were coated in a non-covalent physisorption process with 0.25 mg/ml of NeutrAvidin Biotin Binding Protein (Pierce) in PBS for 30 min at room temperature. The device was washed three times with PBS and one time with distilled water, and dried using nitrogen. The biotin labeled 204-4 mAb was adsorbed to the NeutrAvidin Biotin Binding Protein at 0.25 mg/ml in PBS for 30 min at room temperature. For the detection of SNV, anti-SNV-G1 scFv at 0.25 mg/ml was directly adsorbed to the SAW device for 30 min at room temperature. After coating with the antibodies, the biosensor devices were washed three times with PBS and one time with distilled water, followed by nitrogen drying.

2.4. SAW detection of Coxsackie and SNV

For display and acquisition of the digitized voltage data from the sensor platform, a custom LabVIEW (National Instruments; www.ni.com) program was developed. The data from each of the delay lines were acquired simultaneously and the voltage information was converted back to the phase. Data from the reference line were subtracted from the data from the test lines for each time point measured and continuously saved to disk in spreadsheet format. The data for the quantitative measurements of viral detection presented in this study refer to the phase differential mass shift ($\Delta\varphi$) and are displayed on a graph as a function of time of acquisition. Multiple data points per time are recorded during this process. The SAW device was assembled in a static cell with a 325 MHz input frequency from a power supply. The chamber (fluidic housing) was covered with 0.4 ml of PBS or medium and the phase differential was stabilized for at least 100 s. 0.1 ml of solution was removed and replaced with 0.1 ml of virus containing solution. Virus was typically detected within ∼15 s as observed by an elevation of the signal $\Delta\varphi$ (in degrees on the *y*-axis) along the time plot (*x*-axis). The detection run was allowed to reach stabilization of the phase differential, typically after ∼2 min. The virus containing solution can be removed and the run can be continued with 0.4 ml of PBS until stabilization. $\Delta\varphi$ can either be measured at stabilization after agent injection or after removal of the agent and re-stabilization in buffer. A detailed description of the former process is given in Fig. 2.

2.5. Statistics

All phase differential mass shift ($\Delta\varphi$) data points were generated in at least duplicate and sometimes up to five tests. Data is presented as average ± standard errors (S.E.). The statistical difference between groups of average measurements of phase differential mass shifts $\Delta\varphi$ were determined using the Student's *t*-test. $p < 0.05$ was considered to be statistically significant.

3. Results

3.1. Initial testing of the SAW detector

The major objective of this study was to couple the characteristics of SAW with the selectivity of antibodies to detect viruses of high medical and bio-warfare importance. Fig. 1A depicts the overall schematic concept of our device. Fig. 1B shows the miniature size of the wafer sensors, i.e. approximately

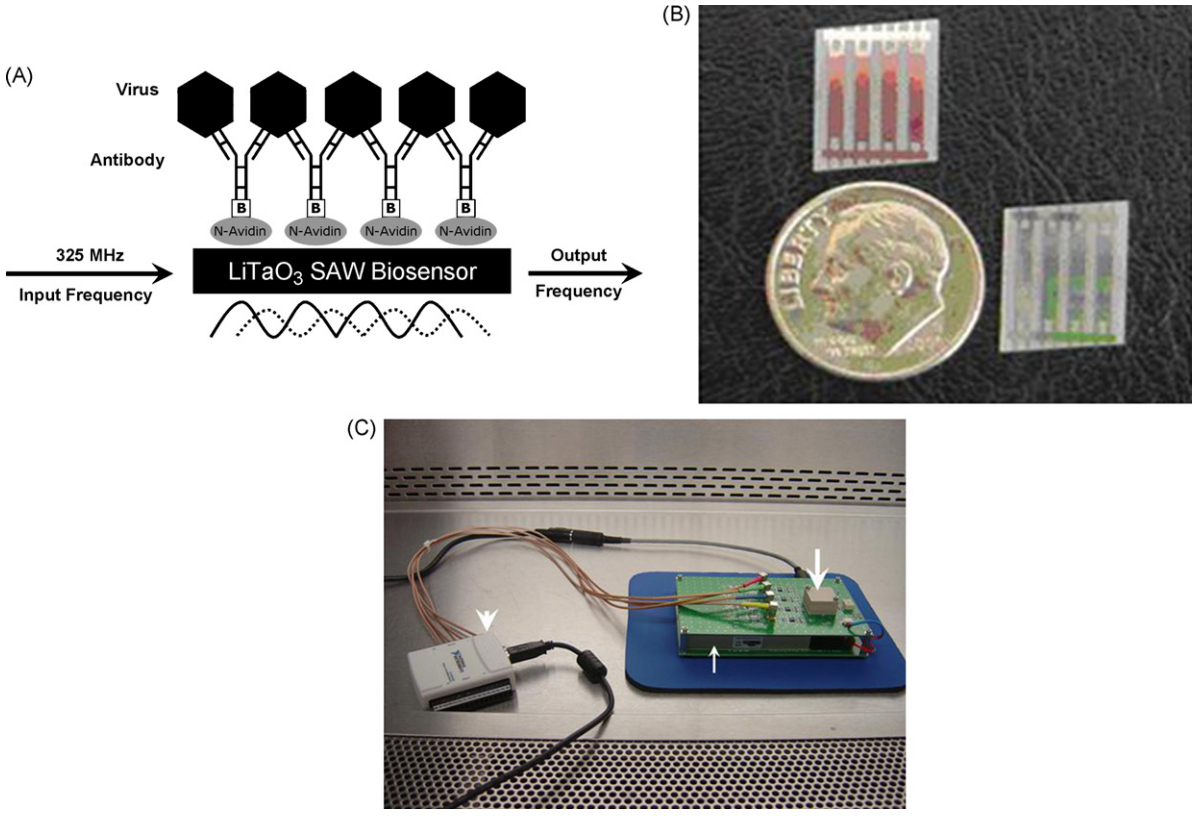

Fig. 1. (A) Concept of the antibody-based virus surface acoustic wave (SAW) biosensor. The lithium tantalate ($LiTaO_3$) sensor surface was coated with NeutrAvidin Biotin Binding Protein (N-Avidin) and coupled to biotinylated [B] monoclonal anti-JVB antibody for Coxsackie virus. Anti-SNV-G1 glycoprotein scFv antibody for SNV detection was coupled directly. Molecular interaction between virus and antibody elicits an acoustic wave leading to a change in the input frequency of 325 MHz. (B) The sensor wafer is shown in scale compared to a dime coin (10 US cents); four aluminum delay lines are visible; one serves as the reference and three as the test delay lines. (C) The SAW detection board (thin arrow) with the fluidic housing (thick arrow) and the output interface device (arrowhead) to a laptop computer is shown.

15 mm × 20 mm, featuring four delay lines, of which one is used as the reference line, while the others are used as test lines. Fig. 1C shows the SAW detection board with the fluidic housing (containing the wafer) and the output interface device to a laptop computer. The sealed fluidic housing connected the IDTs to the electrical input/output system of the static cell; a power supply provided an input frequency of 325 MHz. The phase differential mass shift $\Delta\varphi$ (expressed in degrees) was captured on the laptop computer using a custom LabVIEW program.

Viral detection was performed by immobilizing antibodies onto the sensor. The test delay lines were either directly coated with unlabeled antibodies (for SNV) or with NeutrAvidin Biotin Binding Protein followed by biotinylated antibodies (for Coxsackie virus B4). Fig. 2 represents a typical phase differential plot generated by exposing the sensor to 1.8×10^4 SNV particles/μl. The plot shows the PBS buffer calibrated surface at ∼50°, injection of the virus containing solution at ∼280 s (measured on the *x*-axis), and maximal signal at ∼420 s (∼2 min after agent injection). Detection was evident at ∼15 s after addition of the agent and resulted in an overall $\Delta\varphi$ of ∼5° (measured on the *y*-axis). Thus, $\Delta\varphi$ can be measured shortly after agent injection and the overall process can be performed within minutes. All subsequent data for the quantitative measurements of viral detection refer to the change in $\Delta\varphi$ as described in Fig. 2.

3.2. Quantitative and selective detection of Coxsackie B4 and Sin Nombre virus (SNV)

The SAW biosensor was used in a series of experiments for the detection of Coxsackie virus B4 particles (Fig. 3). Increasing concentrations of viral particles ranging from 9×10^5 to 3.6×10^6 viruses/μl were analyzed as described in Fig. 2. $\Delta\varphi$ was recorded for each concentration and resulted in a dose-dependent increase with $\Delta\varphi$ values ranging from 0.95 ± 0.54 to 6.99 ± 0.96 (Fig. 3; data set to the right). There was a linear relationship between viral load and $\Delta\varphi$ for this range of viral particles with a correlation coefficient R^2 of 0.99. To determine the selectivity of the biosensor for its target in the presence of a confounding agent, the experiments were repeated using admixtures of Coxsackie B4 and HSV-1 viruses. HSV-1 was spiked into the Coxsackie virus preparations at equal final concentrations as for Coxsackie B4 and the previous experiments were repeated. HSV-1 did not affect the selectivity for Coxsackie B4, yielding similar $\Delta\varphi$ values ranging from 1.09 ± 0.66 to 7.24 ± 0.36. The relationship between viral load and $\Delta\varphi$ remained linear with a correlation coefficient R^2 of 0.98. In these spiking experiments, where HSV-1 was used as a confounding agent, the $\Delta\varphi$ for HSV-1 at a concentration of 3.6×10^6 μl^{-1} was 0.64 ± 0.33, indicating that the biosensor did not detect HSV-1.

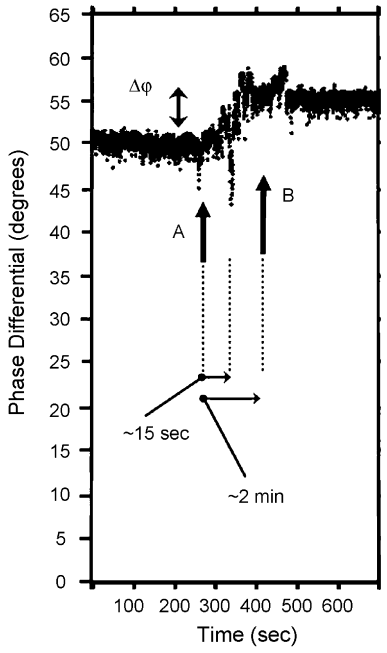

Fig. 2. Representative SAW biosensor plot showing the response to 1.8×10^4 SNV particles/μl. Output was captured using a custom LabVIEW (National Instruments; www.ni.com) program. The data is reported as phase differential mass shift $\Delta\varphi$ (indicated by double-headed arrow) on the *y*-axis as a function of time on the *x*-axis, corresponding to the maximal difference between buffer-calibrated phase differential before addition of agent (arrow A at ~280 s) and after stabilization of signal (arrow B at ~420 s). Dotted lines indicate detection at ~15 s and maximal signal difference at ~2 min after addition of the agent. Single vertically oriented data points are visible as a function of time. See text for details.

Next, we used the SAW biosensor to detect an agent of high medical concern, i.e. SNV, a member of the hantavirus *genus* of the family *Bunyaviridae* and an NIH-designated bioagent of category A (Bronze et al., 2002). Concentrations of 1.8×10^1 to 1.8×10^4 viral particles/μl resulted in $\Delta\varphi$ of 0.63 ± 0.49 to 4.85 ± 0.77 (Fig. 3; data set to the left). The measured values displayed variation with some overlap as shown by their standard errors. This can be attributed mainly to factors related to microfabrication reproducibility for the current sensor system. Our studies indicate that sensitivity is a function of the absolute thickness of the silicon dioxide waveguide. We have determined that thickness variations of 5% lead to a ~8% alterations in detection sensitivities (data not shown). However, our calculated waveguide variations for the current sensors are approximately 1–2%, which is unlikely to contribute to the observed experimental variation. In addition, variations in the lithographic process which guides the geometry of the IDTs on our sensors can influence their sensitivity. We are currently gathering data to quantify this potential problem and may change the process from contact to projection lithography. Nevertheless, the data means resulted in a linear relationship between viral load and $\Delta\varphi$ for this range of viral particles with a correlation coefficient R^2 of 0.95. Similar to the experiments with Coxsackie virus, the selectivity of the SAW biosensor for SNV was not diminished by the presence of confounding HSV-1 at equal concentrations. The corresponding $\Delta\varphi$ ranged from 0.78 ± 0.30 to 4.83 ± 1.36 and the relationship between viral load and $\Delta\varphi$ remained linear with a correlation coefficient R^2 of 0.97. For this set of experiments, the biosensor was marginally sensitive to HSV-1 alone, resulting in $\Delta\varphi$ values of 0.56 ± 0.27 and of 1.51 ± 0.40 for viral concentrations of 1.8×10^3 and 1.8×10^4 μl^{-1}, respectively.

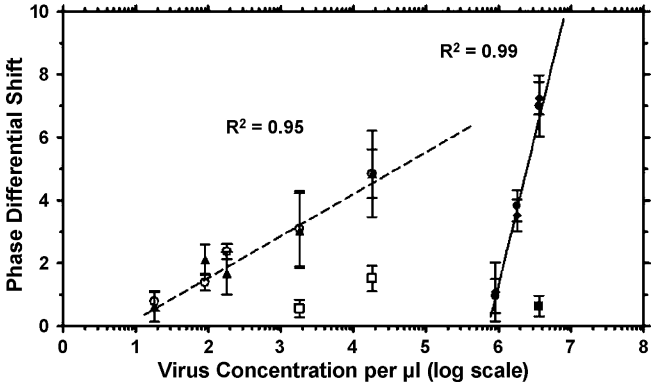

Fig. 3. Detection of Coxsackie virus B4 and SNV using the SAW biosensor. Data was acquired as described in Fig. 2 and in the text. The plots show the shifts in phase differential (°) on the *y*-axis as a function of increasing viral particle concentrations (in virus/μl) on the *x*-axis. Each data point represents an average of 2–5 measurements ± standard errors. (●) Coxsackie virus B4; (♦) Coxsackie virus B4 + HSV-1; (■) HSV-1 alone for the Coxsackie virus experiments; (▲) SNV; (◯) SNV + HSV-1; (□) HSV-1 alone for the SNV experiments. The solid and dotted lines represent the best-fit models and coefficient correlations (R^2) for Coxsackie virus B4 (●) and SNV (▲), respectively.

Based on the lowest concentrations tested for both viral agents, which in both cases yielded $\Delta\varphi$ above values obtained with HSV-1, the sensitivity for the antibody directed against SNV was approximately 5×10^5-fold greater compared to the sensitivity of the antibody directed against Coxsackie B4 virus. The slopes for the detection of Coxsackie virus and SNV were markedly different (Fig. 3). This could be due to multiple factors including the deposition efficiency and corresponding site density of the capturing agents coated on the biosensor surface, in this case the anti-Coxsackie B4 and anti-SNV antibodies, which determines the number of binding sites available to specific viral ligands, in this case the Coxsackie B4 JVB epitope and the SNV-G1 glycoprotein. Similarly, differences in sensitivity can be explained by its dependence on the affinity between an antibody and its corresponding antigen. This leaves room for the development of better immunological tools with higher sensitivities. Accordingly, we are currently employing phage display to identify high affinity protein–peptide interactions to increase the sensitivity for viral particles.

3.3. Virus detection in complex solutions

The SAW biosensor was applied to a real world scenario which could mimic the exposure of an urban population to a viral agent, such as for example through the water system. In these proof-of-principle experiments, SNV particles were spiked into 0.4 ml of either the sewage effluent water of the City of Albuquerque NM, water taken from the Rio Grande River in Albuquerque, or distilled water or PBS as controls at

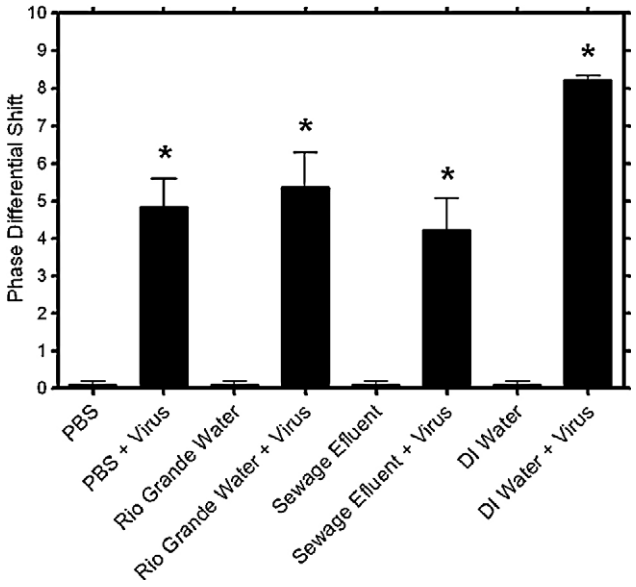

Fig. 4. Detection of SNV in complex solutions using the SAW biosensor. SNV viral particles were spiked into distilled (DI) water, phosphate buffered saline (PBS), sewage effluent, or Rio Grande water for a final concentration of 1.8×10^4 viral particles/μl. Data was acquired as described in Fig. 2 and in the text. The plots show the shifts in phase differential (°) on the *y*-axis as a function of solution input on the *x*-axis. Each data point represents an average of two measurements ± standard errors. Stars denote statistical significance ($p < 0.05$) over background (no virus) solutions using Student's *t*-test.

a final concentration of 1.8×10^4 virus/μl. As shown in Fig. 4, all of the control solutions lacking viral particles showed similar background levels of $\Delta\varphi$ in the order of 0.1. The SAW biosensor showed the highest sensitivity when the viral particles were spiked into distilled water, displaying a $\Delta\varphi$ of 8.21 ± 0.11 (∼82× over background). The $\Delta\varphi$ for virus spiked into PBS, Rio Grande River water, and sewage effluent water were similar, i.e. 4.85 ± 0.77, 5.36 ± 0.93, and 4.22 ± 0.84, respectively, corresponding to ∼48×, 54×, and 42× fold differences over background, respectively. The $\Delta\varphi$ values of all virus spiked solutions were significantly ($p < 0.05$) higher than their background solutions without virus, as determined by Student's *t*-test. In addition, these experiments in complex solutions collectively indicate a high re-usability of the sensor resulting in reproducible data. The data in Fig. 4 represent duplicate experiments using regenerated sensors after treatment with organic solvents, ultrasound, and UV-ozone. Nevertheless, multiple antibody re-coating and re-testing procedures led to $\Delta\varphi$ measurements for the specific target within standard errors of ∼13% of the mean.

4. Discussion

Antibody-based detection by SAW has previously been reported for cellular microorganisms, such as bacteria. We recently reported on a 103 MHz operated SAW sensor to detect bacterial spores of *Bacillus thuringiensis*, a pathogen simulant for *Bacillus anthracis*, at or below inhalational infectious levels (Branch and Brozik, 2004). In that study we developed suitable chemistries to orient the antibodies on the sensor using protein G on two different waveguide materials, i.e. polyimide and polystyrene. We found that polyimide had a lower mass detection limit leading to highly selective bacterial detection as shown by the absence of binding to the control agent *Bacillus subtilis*. Similarly, Berkenpas and colleagues recently described a SAW biosensor that was coated with a polyclonal antibody specific for the toxigenic *Escherichia coli* O157:H7 bacterium which causes hemorrhagic colitis and hemolytic uremic syndrome (Berkenpas et al., 2006). These authors reported $\Delta\varphi$ responses of approximately 14° representing a sevenfold difference over background control antibodies against trinitrophenyl (TNP) hapten.

In contrast, detection of viral agents by antibody coupled SAW is largely absent from the literature. In one of the few published studies Tamarin and colleagues developed a SAW sensor similar to the one presented here, and used it to study physical parameters of specific binding between antibodies and M13 bacteriophages (Tamarin et al., 2003). In addition, Tassew and Thompson reported on the detection of the human immunodeficiency virus (HIV) type 1 Tat protein using immobilized trans-activation-responsive RNA elements and various Tat peptide fragments (Tassew and Thompson, 2003). Thus, our study represents a contribution to the field of specific detection of viral agents by the SAW technology based on protein interactions (antibodies).

Collectively, our experiments using Coxsackie B4 and SNV indicate a high sensitivity and selectivity of the SAW detector for its targets. Importantly, selectivity was not compromised by the presence of confounding and related factors, such as other viruses, indicating the potential use of this device for the specific detection in complex solutions. In a previous study we have used quantitative (real time) reverse transcriptase polymerase chain reaction (RT-PCR) specific for the S segment of SNV RNA to determine viral copy number in bodily fluids, such as blood plasma and tracheal aspirates (Xiao et al., 2006). Assay sensitivity was ∼5000 RNA copies (corresponding to viral particles) per ml, but the material to be tested had to be processed. Pre-processing of analyte is also necessary for other established techniques, including enzyme linked immunosorbent assay (ELISA) and surface plasmon resonance (SPR). Furthermore, SPR technology is still relatively costly and not amenable to a portable format. In contrast, our SAW platform allows detection of viral bioagents without pre-processing of the analyte, and can be developed into a portable field application. The SAW biosensor was able to detect at least 7000 SNV particles. Although the minimal infectious dose of SNV necessary to establish a successful human infection remains unknown, this number is substantially lower than the dosage found in hantavirus infected humans suffering from HCPS (Xiao et al., 2006).

An important and novel finding of this study is the detector's application to a real world scenario using water obtained from the sewage system and from a river of an urban area. This is a real world possibility for planned or accidental bioagent distribution and can lead to mass exposure within the population, which in turn can lead to an extensive health crisis (Bronze et al., 2002; www.cdc.gov). Naturally occurring water bodies,

such as rivers are admittedly very complex solutions containing perhaps millions of different organic and inorganic molecules. It is thus noteworthy that our antibody-coated biosensor was able with high selectivity to detect the correct agent against this complex background. While the likelihood of detection in a large body of water could be increased by concentration strategies, such a procedure would compromise two important strengths and advantages of the current system, i.e. the hand-held, portable nature, and the absence of analyte pre-processing. In addition, it remains to be shown whether a flow-through set-up that continuously monitors dilute samples vs. the static set-up reported here would increase the representative power of the analyzed sample. In a static setting changes in phase differential due to the added agent and buffer are accumulating, while in a flow-through setting the sensor would return back to the original phase differential of the carrier buffer, as the sample passes through the sensor. Comparisons between these approaches are currently under investigation in our laboratory.

Together, these data indicate that our sensor may be used under field conditions and warrant further efforts into the development of inexpensive portable devices for field operation. Towards this end, we are currently working on a hand-held battery operated and thus self-contained version.

5. Conclusions

Detection of biological agents and their products in the context of bio-warfare and human health is an important task with a current sense of urgency. Applications include the detection of agents and their products in the environment after planned or accidental distribution into the soil or water bodies, such as swimming pools, rivers, aquifers, and the sewage system, especially in highly urbanized areas. Another application is the detection of agents and markers thereof in human fluids and tissues for the correct diagnosis and treatment stratification of patients. Towards this end, we have developed a SAW biosensor that is capable of rapidly detecting viral agents with high selectivity and sensitivity for at least two different targets, i.e. Coxsackie B4 virus and the category A bioagent SNV. Our detector combines the sensitivity of surface acoustics with the selectivity of antibody–antigen recognition and offers a highly versatile platform for the detection of other viral agents and their products. Further, the results obtained in this study emphasize the possibility for future, more refined developments and applications of portable SAW-based technology in the fields of viral medicine and environmental surveillance.

Conflict of interest

No author has a conflict of commercial interest in this study.

Acknowledgements

This work was conducted with support from the National Science Foundation, grant number IIS-0434120, and from NCMR to Dr. Richard S. Larson, and from the National Institute of Allergy and Infectious Diseases, grant numbers UO1 AI56618 and UO1 AI054779 to Dr. Brian Hjelle. Mrs. Jacquelyne Tuck, Grants Coordinator at the University of New Mexico School of Medicine Department of Pathology is greatly acknowledged for excellent administrative support. We thank Dr. Stephen Young from TriCore Laboratories (Albuquerque, NM, USA) for providing purified and tittered Herpes Simplex virus type 1.

References

Berkenpas, E., Millard, P., Pereira da Cunha, M., 2006. Biosens. Bioelectron. 21, 2255–2262.
Branch, D.W., Brozik, S.M., 2004. Biosens. Bioelectron. 19, 849–859.
Bronze, M.S., Huycke, M.M., Machado, L.J., Voskuhl, G.W., Greenfield, R.A., 2002. Am. J. Med. Sci. 323, 316–325.
Deisingh, A.K., Thompson, M., 2004. Can. J. Microbiol. 50, 69–77.
Frydenberg, A., Starr, M., 2003. Aust. Fam. Phys. 32, 594–595.
Hjelle, B., 2002. Expert Rev. Vaccines 1, 373–384.
Jay, M., Ascher, M.S., Chomel, B.B., Madon, M., Sesline, D., Enge, B.A., Hjelle, B., Ksiazek, T.G., Rollin, P.E., Kass, P.H., Reilly, K., 1997. Emerg. Infect. Dis. 3, 183–190.
Martin, F., Newton, M.I., McHale, G., Melzak, K.A., Gizeli, E., 2004. Biosens. Bioelectron. 19, 627–632.
Mertz, G.J., Hjelle, B., Crowley, M., Iwamoto, G., Tomicic, V., Vial, P.A., 2006. Curr. Opin. Infect. Dis. 19, 437–442.
Moll, N., Pascal, E., Dinh, D.H., Pillot, J.P., Bennetau, B., Rebière, D., Moynet, D., Mas, Y., Mossalayi, D., Pistré, J., Déjous, C., 2007. Biosens. Bioelectron. 22, 2145–2150.
Palacios, G., Oberste, M.S., 2005. J. Neurovirol. 11, 424–433.
Tam, P.E., 2006. Viral Immunol. 19, 133–146.
Tamarin, O., Comeau, S., Dejous, C., Moynet, D., Rebiere, D., Bezian, J., Pistre, J., 2003. Biosens. Bioelectron. 18, 755–763.
Tassew, N., Thompson, M., 2003. Org. Biomol. Chem. 1, 3268–3270.
Velappan, N., Martinez, J.S., Valero, R., Chasteen, L., Ponce, L., Bondu-Hawkins, V., Kelly, C., Pavlik, P., Hjelle, B., Bradbury, A.R., 2007. J. Immunol. Methods 321, 60–69.
Xiao, R., Yang, S., Koster, F., Ye, C., Stidley, C., Hjelle, B., 2006. J. Infect. Dis. 194, 1403–1409.